

Enhancing Bifacial PV Efficiency With the Addition of a Rear Side Reflector

By: Neila Watson

Submitted in Partial Fulfillment of the
Mechanical Engineering Honors Bachelor's Degree

Faculty Advisor: Professor Richard Wilk

Union College

Mechanical Engineering Department

MER-498

Class of 2022

Abstract

Bifacial photovoltaics are an expanding sector of solar electricity production, collecting solar energy on the front, back, and sides of the module. This increases the efficiency by around 10% to 30% over a typical mono facial cell, which only collects sunlight on the front. However, the performance of bifacial PV arrays depends on a variety of factors, including temperature, shadows, solar insolation, and set-up geometry. The geometry is affected by the tilt angle, the azimuth angle, the height from the ground to the panel, and the reflectance from the ground surface. The addition of a reflector, usually white in color to reflect sunlight, further complicates a PV configuration. When a reflector is added to face the backside of a collector, the set-up can then be enhanced to increase the bifacial gain, or the ratio of rear side energy to the front side. This paper will use a numerical model through the Python coding language to determine the incident energy on both sides of a bifacial collector. The computational model could then be verified through data gathered from an experimental setup using smaller PV cells to simulate the backside of a bifacial collector. Then by combining both the experimental and computational data, an indoor, sized-down model could be used during the winter months. The computational model was helpful in verifying trends found through experimental data. A 1 m reflector-collector distance in the outdoor model to found to significantly increase the energy collected by 20%. Nonuniformity between the rows was observed as the reflector was moved closer, due to a lower view factor. There is an optimal distance where BG peaks, then the BG plateaus when moved further. Because a large variety of factors contribute to the set-up of PV arrays, many tests need to be conducted, and the optimal arrangement is difficult to decipher.

Table of Contents

Abstract

List of Figures 4

Acknowledgments 5

Introduction 6

Background and Literature Review 9

Model and Experiments 14

Results and Discussion 23

Conclusions 33

References 35

Appendices 37

List of Figures

Figure 1: Schematic of the experimental setup used by Cuevas et al. [5]

Figure 2: Minimum value of albedo where vertical mounted bifacial panels perform better than monofacial farms [11].

Figure 3: Open rack set up with a white rear-side reflector [12].

Figure 4: Schematic of reflector-collector set-up.

Figure 5: Solar module used to simulate the rear side of a bifacial collector.

Figure 6: Schematic of the outdoor collector with seven cells mounted.

Figure 7: Daily trend of sunlight measurement from pyranometer.

Figure 8: Cell voltage plotted against pyranometer W/m^2 to get calibration value.

Figure 9: Set-up of cells on the collector.

Figure 10: Reflector-collector set-up with a separation distance of 1m.

Figure 11: Schematic of the indoor collector with four modules.

Figure 12: Indoor bifacial PV reflector-collector set-up.

Figure 13: Indoor bifacial PV reflector-tilt set-up.

Figure 14: Indoor bifacial PV additional white ground reflector set-up.

Figure 15: Indoor bifacial PV Mylar film reflector set-up.

Figure 16: Diagram of altitude and azimuth angle to a PV panel [14].

Figure 17: Bifacial gain of 3 cells found experimentally with no reflector.

Figure 18: Bifacial gain of 3 cells found experimentally with 1m reflector distance.

Figure 19: Computational results for the bifacial gain at reflector-collector distances of 0.5, 0.75, and 1m.

Figure 20: Bifacial gain for a reflector-collector distance of 1 m for the outdoor experimental and computation models.

Figure 21: Bifacial gain for several reflector-collector distances from the indoor model.

Figure 22: Bifacial gain for various reflector-collector distances showing a peak then plateau for both the indoor and computation models.

Figure 23: Bifacial gain for top and bottom row of modules over peak solar time with a 1m reflector-collector distance outside.

Figure 24: Bifacial gain for top and bottom row of modules over a range of reflector-collector distances inside.

Figure 25: Bifacial gain of each of the four cells as the white rear-side reflector was tilted.

Figure 26: Bifacial gain of each of the four modules with and without a white ground reflector.

Acknowledgments

I would like to thank my thesis advisor Professor Richard Wilk, as well as the Mechanical Engineering Department at Union College.

Introduction

Solar energy is gaining more popularity across the nation, due to being renewable energy and the fact that it is a pollution-free source of power. In order to increase the production efficiency of typical photovoltaic cell applications, bifacial PV captures solar energy on both sides of the cell. Average mono facial PV cells work by absorbing sunlight on one side and converting that energy to electricity. Solar-thermal energy can be used for a variety of applications, including water heating, heating buildings, and solar furnaces. Unlike fossil fuels and some other alternative energy sources, solar energy does not release harmful pollutants and can even produce a return on investment. Currently, this is a crucial area of research as bifacial PV is expected to account for half of the PV market in 5 years

A developing adaptation of PV cells can be seen in bifacial photovoltaic cells. Bifacial solar panels use both sides of the module to collect energy and produce electricity, ultimately increasing the amount of energy that can be harvested. Simply, bifacial cells work by increasing the production of electricity per square meter by using light absorption from the ground albedo through a transparent or glass back sheet rather than a typical white back sheet [1]. Different variables affect the geometry of how solar panels are mounted, including the tilt angle, the azimuth angle, the height from the ground to the panel, and the reflectance off of the ground. The tilt angle is defined as the angle of the PV modules from the horizontal surface, whereas the azimuth angle refers to the angle of the panel relative to the south direction. The height from the ground to the panel is the height from the bottom of the panel to the ground. Lastly, the reflectance off the ground is simply the proportion of the solar light that is reflected after striking the ground.

Additional key terms essential to studying solar energy and PV module geometry are defined as follows. Albedo is an important term, defined as the fraction of incident light that is reflected by a surface. Albedo can vary depending on the material of the site and is measured with a pyranometer or a PV module and can be affected by environmental conditions. However, reflectance only refers to visible light, while albedo refers to the entire spectrum of light [2]. Insolation refers to the amount of solar radiation hitting an area. Sunlight striking an object can be broken into the beam and diffuse light. The beam radiance refers to direct sunlight, and the angle of incidence can matter. Diffuse sunlight is any light that is scattered, including any beam or diffuse light from the sky or that is reflected off of the ground. In terms of bifacial PV modules, most of the light that is captured on the rear side comes from diffuse light. However, in the summer when the sun is very high in the sky, direct sunlight beams can be caught. The addition of a reflector, which can be white or even a mirrored surface, can increase the percentage of diffuse and ground reflected light that is then captured by the bifacial, or even mono facial panel.

The efficiency of bifacial cells can be measured by the bifacial gain (BG), measured using Equation 1,

$$\text{Bifacial Gain (BG)} = \frac{\text{Rear Energy}}{\text{Front Energy}} \quad (1)$$

and measures the amount of energy captured on the back of the cell divided by the energy from the front of the cell. The higher the BG the more effective the bifacial panel is. The variables outlined above can be manipulated in order to increase the BG of bifacial solar panels. A variety of combinations of these factors can be studied and tested, but doing so is time-consuming and it is difficult to optimize several different variables through experimentation. Testing a variety of variables would require countless different tests over the course of a year, as the sun's path

changes. Therefore, computational modeling would help add to experimental data, without as much time and cost.

Overall, this report focuses on enhancing bifacial collection by studying the distance from the panel to a white reflector, as well as observing the effects of tilting the rear-side reflector and the addition of a white ground reflector. The effect of reflector-collector distance can be examined by collecting experimental data with the reflector at a variety of different distances from the panel and recording the bifacial gain. Then experimental data is compared to results from a Python model of bifacial PV panels [3]. The data collected from the 6 module set-up outdoors supplemented with the computational model can help in building an indoor, scaled-down model. The indoor model also has two rows of two modules each, also simulating the rear side of a bifacial collector. Different elements can negatively impact the efficiency of the panels, and if one cell is negatively impacted, the entire panel will become less effective. Specifically, non-uniform shading, as well as hotter temperatures, can disproportionately and negatively impact different cells in a PV module, decreasing the performance of a PV panel [4]. Building on research done over the past year, and further studying bifacial photovoltaic panels, we can improve a clean and renewable source of energy.

Background and Literature Review

Bifacial photovoltaic cells have been studied since the 1960s, but have become a major focus in more recent years. The gaining popularity is due to the bifacial module's ability to be illuminated on both sides, and reduce the cost of electricity generated by typical mono facial panels [4]. Bifacial panels were first used in space applications for low-orbiting satellites [6]. More recently, one study by Cuevas et al. was performed in a lab [5]. A bifacial panel was set up within wooden boards painted white in a high-albedo area, sitting alongside a traditional mono facial panel, as seen in Figure 1 [5]. The results ended up showing that the ratio of the bifacial to conventional panels was around 1.5, implying that the bifacial panel was 50% more efficient, even when not exposed to complete sun.

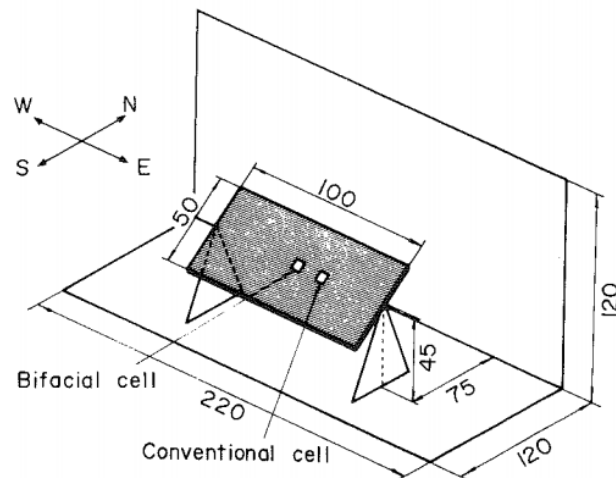


Figure 1: Schematic of the experimental setup used by Cuevas et al. [5]

However, such a high power gain is difficult to attain in a non-laboratory setting, and bifacial panels implemented in real use tend to have a power gain of around 10% to 30% [7]. Tests to determine the optimal performance of bifacial modules have been performed across the globe. The geometry of the set-up, including the tilt angle and orientation, paired with desired

environmental conditions, albedo, and irradiation intensity, can be tested through experiments and numerically [7]. The ideal combination of these parameters depends on the location as well as the time of year. One important finding was that “increasing the ground albedo to 0.5 can boost the bifacial gain of ground-mounted modules to ~20% globally” [7]. However, elevating a solar module 1m off the ground can increase installation cost, but the tradeoff of being too close to the ground can increase the temperature of the module, thereby decreasing performance. When bifacial panels have a lower temperature coefficient, they perform better in high-temperature regions [10]. The lack of a black backing on bifacial panels lowers the temperature that is absorbed by the cell as compared to monofacial panels. Overall, the levelized cost of electricity (LCOE), the average net present cost of electricity generation over the lifetime of large-scale bifacial PV farms, is already less than farming fossil fuels in many cases [7].

Many different set-ups of bifacial PV farms exist, and many have been tested. Different geometries have a variety of benefits and downfalls. In one study done by Applebaum et al., three different farm set-ups in Jerusalem, Israel were compared [10]. All three set-ups had identical bifacial PV panel type, number of collector rows, collector height, the distance between rows, inverter, and cabling. However, one with panels facing east-west and optimally tilted, one facing north-south vertically, and another deployed east-west and optimally tilted. The farm with the optimally-tilted modules ended up producing 32% more energy than the vertical panels facing north-south [8]. The contribution from incident irradiation ended up being negligible on the rear side of the collector for smaller tilt angles. However, this data is difficult to compare to monofacial panels and could change if studied in other locations. Vertical farms also have the added benefit of reducing the presence of dirt or snow, which can be costly to clean and increase energy production. As well as using less ground space than tilted bifacial panels, the tilted panels

need to be elevated off of the ground, adding to cost. A row spacing of 2 m in vertical farms produces the largest energy yield over mono-facial farms but is smaller compared to stand-alone panels [8].

In one study, a MATLAB simulation was developed to compare a vertically mounted bifacial farm compared to a conventionally mounted mono-facial farm [11]. It was found that the latitude, the diffuse factor, and the albedo determine which configuration performed better. The location of the farm determined which set-up would perform better. A mono facial panel captures 100% of the diffuse light from the sky and 0% from the ground in Singapore. Meanwhile, in Germany, a mono facial panel only receives 71% of total diffuse light from the sky and around 29% of diffuse light from the ground in Germany. The average albedo then had to be determined in various countries, and the albedo value resulted in vertical bifacial farms performing better than conventional mono facial farms. These albedo values, found from satellite pictures, can be observed in Figure 2. However, the albedo is more affected by local, rather than global locations

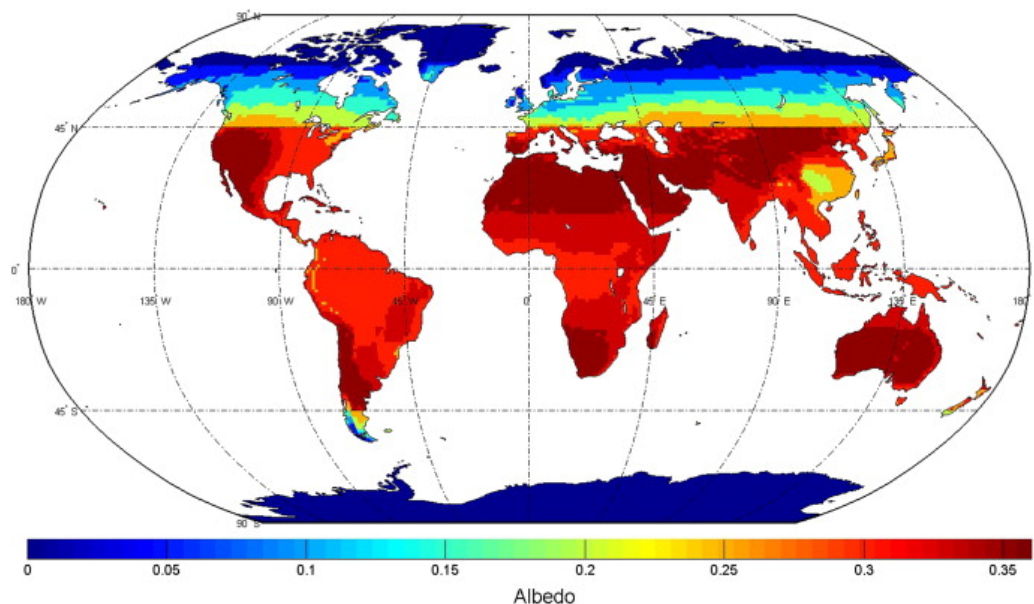


Figure 2: Minimum value of albedo where vertical mounted bifacial panels perform better than monofacial farms.

Lots of work has been done at Union College surrounding bifacial panels and has been built upon throughout this paper. In late 2020 through 2021, Matthew Rueter developed a computational model to accurately predict incident energy on the front and rear of a bifacial panel enhanced with a rear side reflector [3]. Matthew used the Python coding language with Numpy and Matplotlib modules to develop the code. However, the model relies on past historical averages of weather in Schenectady, which is not always accurate to the experimental tests. Nonetheless, the model is versatile and can be applied to different locations and replicate different geometries. Additionally, over the summer of 2021, Matthew Rueter and Mariam Dobosz studied the addition of a rear side reflector, and verified the results from the computational model, using both a white and reflective Mylar film reflector. The white diffuse reflector increased the bifacial gain over no reflector used and was slightly more beneficial than the reflective Mylar film [9]. They brought up the idea that in the summer the reflector would need to be closer to the collector due to larger solar angles, but this could then impact ground reflectance. But in the winter, the reflector could be farther from the collector due to the smaller altitude angles of the sun. These geometric parameters and ideas will be addressed and tested throughout this paper.

Not many indoor bifacial experiments have been performed, however, Lopez-Garcia J., Casado A., and Sample T. conducted both indoor and outdoor experiments using bifacial silicon PV modules with various setups including an open rack or vertical set-up, a structure with baffles or blocks above and below, and an array of three modules next to each other. Then each of the three set-ups were tested with white and non-reflective reflectors behind them at various differences [12]. It was recommended to attach a black cover to the rear side of the panels indoors to maximize accuracy. The power gain was found to be as high as 20% in the open rack

set up with a white reflector as seen pictured in Figure 3 below. Although non-uniformity was found when the I-V or current-voltage graphs were made, the addition of baffles increased uniformity on the rear side [12].

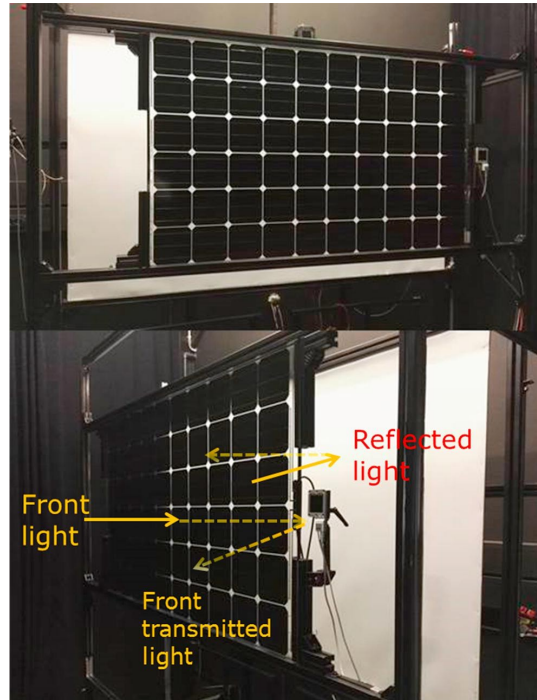


Figure 3: Open rack set up with a white rear-side reflector [12].

When studying the addition of a rear-side reflector behind a bifacial module, the view factor, or “the angular range from which light can reach the module” must be considered [13]. K Jäger et al. studied an illumination model for a large bifacial field, considering diffuse light reflected from the ground. A computational model was developed to assess this phenomenon, and implement equations for the view-factor of each module, rather than using the more complicated method of ray tracing [13]. However, when a model relies on view factors, the irradiance reaching the panels is an average, which overestimates the actual performance. The view factors of bifacial PV cells can be helpful when understanding the patterns in the bifacial gain as a reflector is moved closer or farther from the rear side of a collector.

Model and Experiments

In order to test the effects of a rear side reflector on bifacial modules, different steps had to be taken. In general, a reflector-collector set-up was used, and different separation distances, d , between the two boards were then tested. As seen in Figure 4, the reflector was set up on the backside of the collector. Seven small modules, or 1.0V 400mA, as can be seen in Figure 4, these smaller modules were placed on the backside of the representative collector in order to simulate the rear side of a bifacial collector.

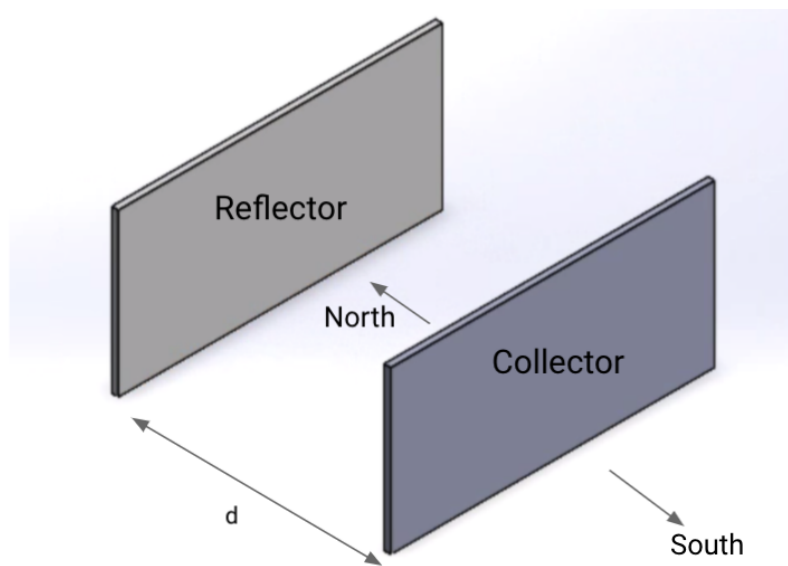


Figure 4: Schematic of reflector-collector set-up.

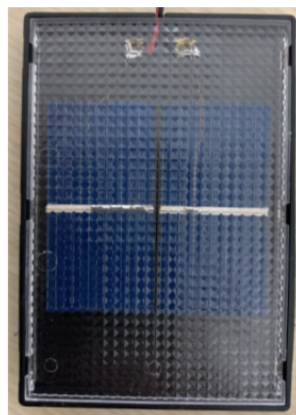


Figure 5: Solar module used to simulate the rear side of a bifacial collector.

In order to begin experiments using the solar modules, each small module had to be calibrated. This was done by mounting the modules on the collector as seen in Figure 6. The collector was then placed in the sun, alongside a pyranometer, to measure the solar insolation. The solar irradiance measured in W/m^2 of the Pyranometer could be measured, as well as the voltage output of each individual cell. The daily trend of sunlight as measured from the pyranometer can be seen in Figure 7, with peaks at around noon solar time each day. The voltage of each cell could then be correlated to the pyranometer W/m^2 to get calibration factors for each individual cell. An example calibration curve for one cell can be observed in Figure 8. This was done by plotting the voltage output of the cell against the W/m^2 from the pyranometer, then fitting a trendline to the graph and finding the calibration factor from the slope of the trendline. In this case, the calibration factor came out to $1379 \text{ W}/\text{m}^2/\text{V}$, with an R^2 value of 0.98. All of the calibrations for the 7 cells can be seen in Appendix A.

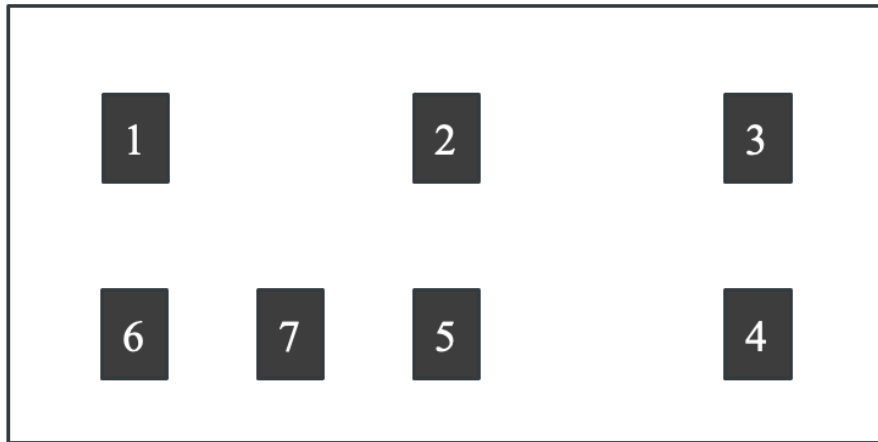


Figure 6: Schematic of the outdoor collector with seven cells mounted.

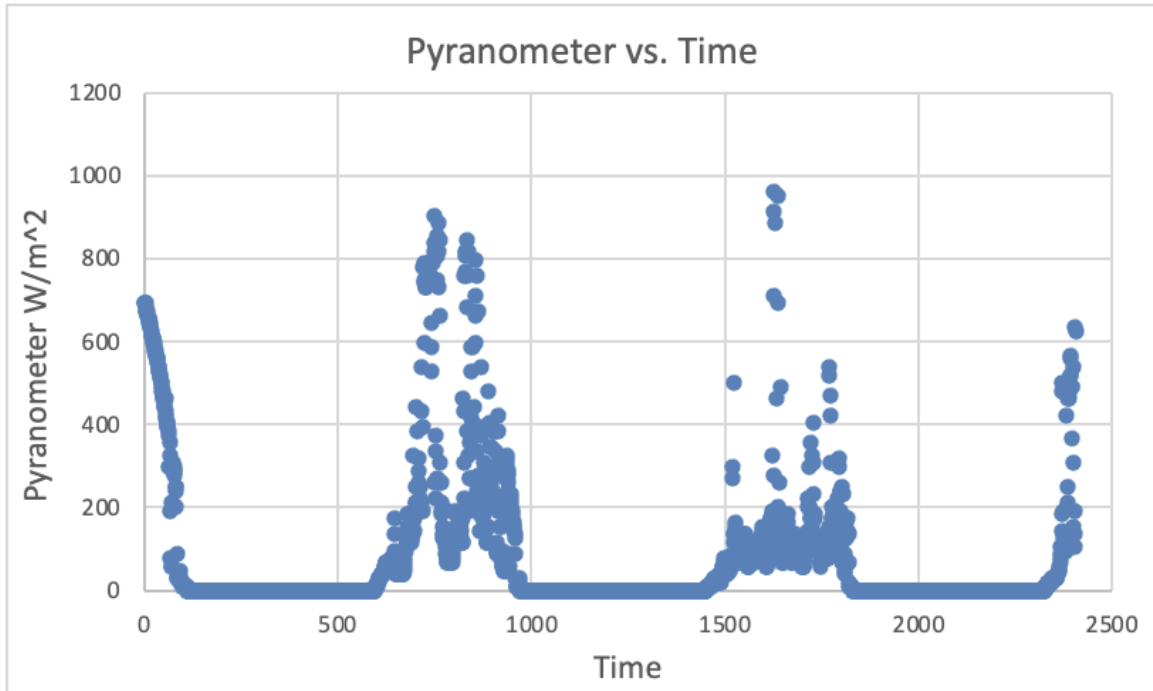


Figure 7: Daily trend of sunlight measurement from pyranometer.

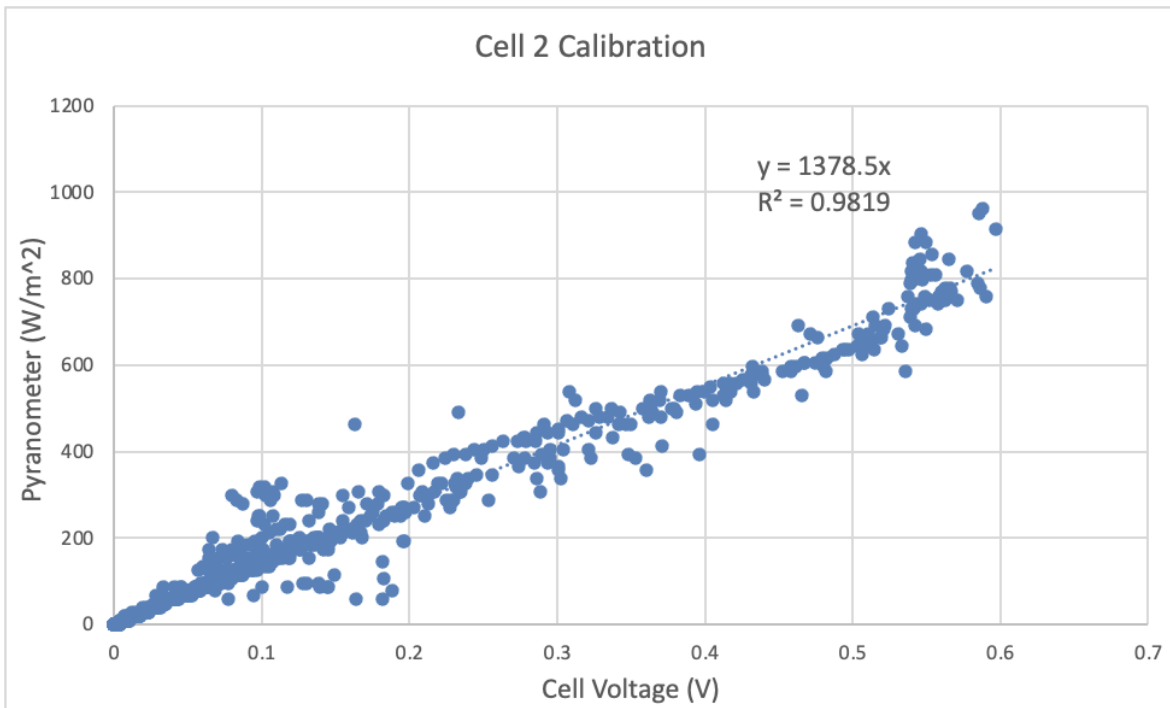


Figure 8: Cell voltage plotted against pyranometer W/m^2 to get calibration value.

Once all of the cells to be used in experiments were calibrated successfully, the collector board was faced to the north, away from the sun (Fig. 9). The pyranometer measured the solar energy to the front of the board. A baseline test was then run without a reflector behind the collector, and just black tarps were laid down behind the collector. A reflector was then added to the backside of the collector, (Fig. 10), where the reflector was placed 1 m from the backside of the collector. The bifacial gain can then be calculated for each cell, or the ratio of the rear energy from the cells to the front, or the side energy as measured by the pyranometer.



Figure 9: Set-up of cells on the collector.



Figure 10: Reflector-collector set-up with a separation distance of 1m.

The bifacial gain with the presence of a reflector was greater than without a reflector. Then the experiments could be run with several different separation distances between the collector and rear-side reflector. These experiments could then be simulated using the computational model and comparing the results. However, the computational model relies on weather averages from Schenectady, which is not entirely identical to the experiments. Nonetheless, the computational model is helpful in comparing and predicting the results of experiments. And doing so quickly, especially as the weather conditions worsen.

In order to continue testing the effects of a rear-side reflector on Bifacial PV efficiency during the winter, an indoor scaled-down model could be constructed. A schematic of the model can be seen in Figure 11, the model was made of wood with dimensions of 13.5 in. by 13.5 in., with two rows of two solar modules.

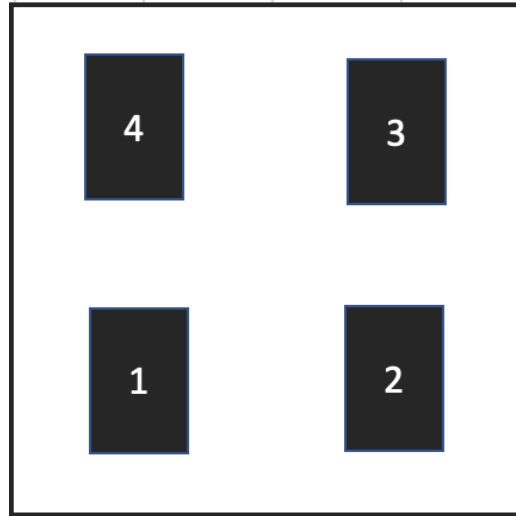


Figure 11: Schematic of the indoor model with four modules.

The overall set-up mirrored that of the outdoor experiment, with cells on one side of a panel, simulating the rear-side of a bifacial collector facing away from the sun, or two lights in the indoor case. Then, a white reflector with the same dimensions as the “collector” was placed facing the modules, simulating the rear side of the reflector. The solar modules do not face the light source, two Luminar Work lights. This setup can be seen in Figure 12. The four cells used had to be calibrated against a pyranometer the same way used for the outdoor model. The indoor model could be used to test many different variables that could not be done outside due to poor weather conditions and time constraints. While the indoor model could be set up in a certain geometry, and the short circuit current of each cell could be recorded and then converted to the solar insolation, W/m^2 , using the respective calibration curve which can be seen in Appendix A.

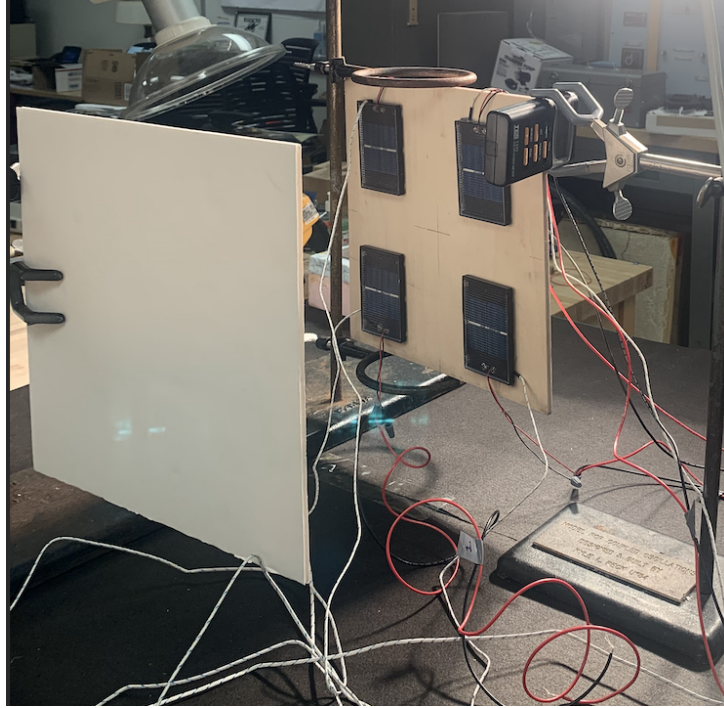


Figure 12: Indoor bifacial PV reflector-collector set-up.

Some other parameters that could be explored inside are the tilt of the reflector, the addition of a white ground reflector, and a mylar film reflector versus white. These set-ups can be seen in Figures 13, 14, and 15 respectively. The results from these various set-ups could give insight into potential changes that could help improve bifacial PV farms. While the indoor model was more time-efficient, the lights used were not as strong as the sun was during the experiments conducted in the Fall. In addition, the lights were much closer to the collector and pyranometer, so there is less diffuse light to be absorbed by the modules or reflected by the surrounding areas and the white reflector.



Figure 13: Indoor bifacial PV reflector-tilt set-up.

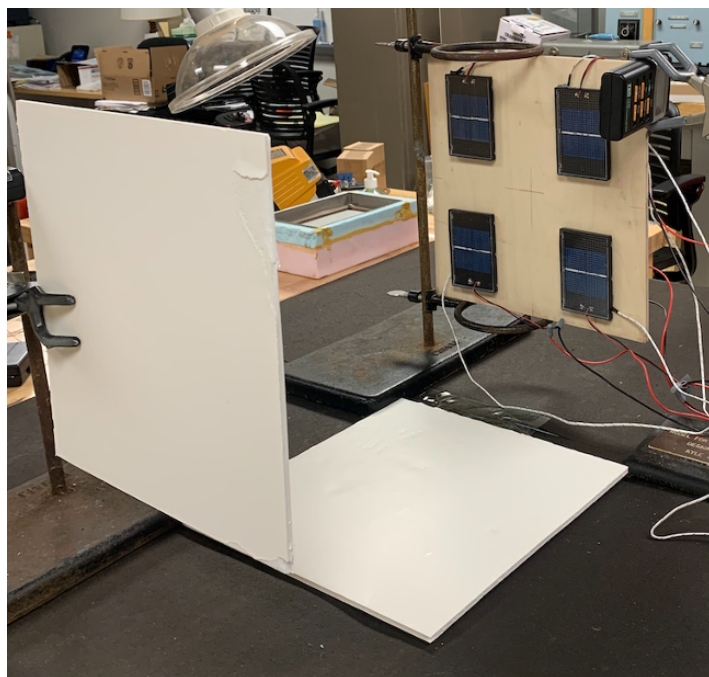


Figure 14: Indoor bifacial PV additional white ground reflector set-up.

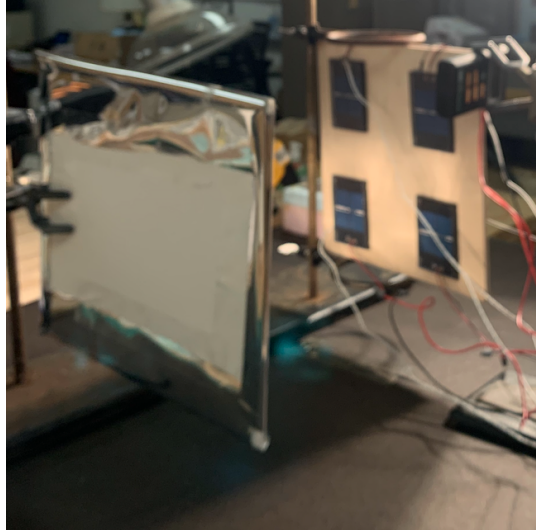


Figure 15: Indoor bifacial PV Mylar film reflector set-up.

The data collected from the indoor model could be compared to the computational model by measuring the altitude angle of the lights to a line orthogonal to the collector, which can be seen in Figure 16. The altitude angle was measured to be 25° , which correlated to the altitude angle of the sun at noon on January 10 in Schenectady. The Python model could then be run with various parameters on that date and compared to results from the indoor model.

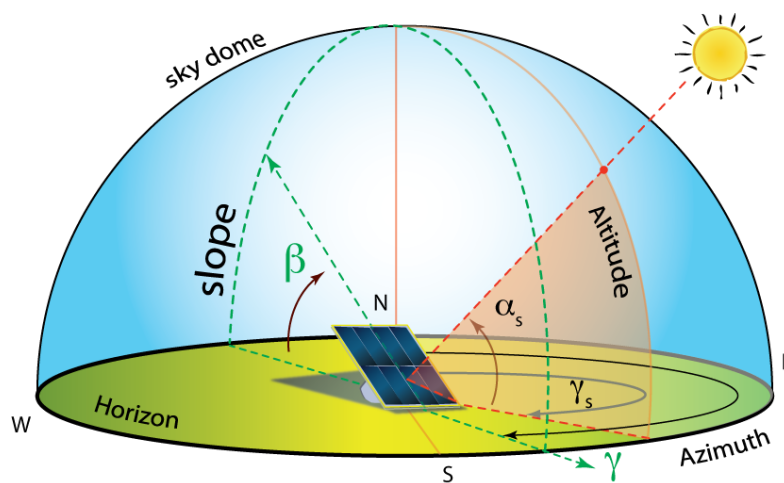


Figure 16: Diagram of altitude and azimuth angle to a PV panel [14].

Results and Discussion

From the experiments described above, after testing the bifacial gain without a reflector, the BG of the top row of three cells was each around 0.15, (Fig. 17). However, with a separation distance of 1m between the collector and backside reflector, the bifacial gain of three cells can be seen plotted in Figure 18. The bifacial gain in all three panels is around the same value, as the three cells were all on the same row. The bifacial gain comes out to around 0.2 or 20%. Therefore, using a reflector was found to be more effective than without a reflector. The separation distance could then be focused on. However, as the reflector is moved closer to the collector, shading might occur, and the view factors are implemented into the computational model to calculate the amount of diffuse light blocked by the reflector or other collectors. At low and high times, irregularities can be seen in Figure 17, possibly due to the shading from metal bars as the sun rises and sets.

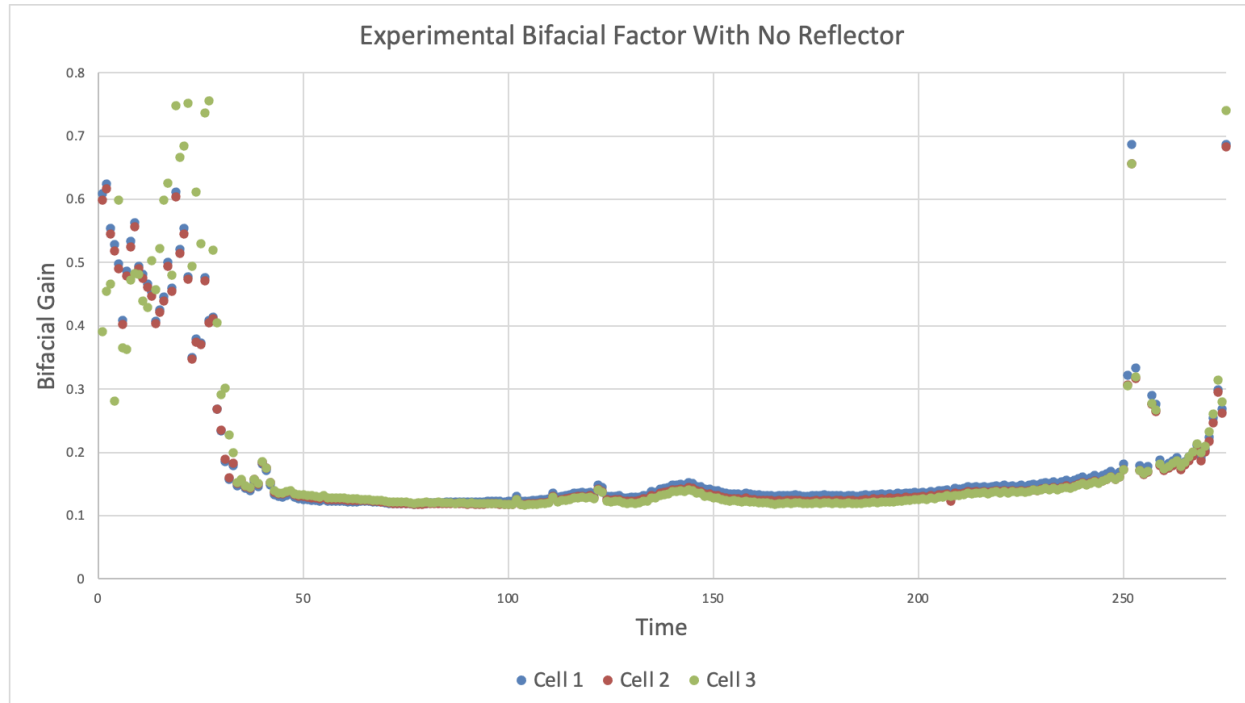


Figure 17: Bifacial gain of 3 cells found experimentally with no reflector.

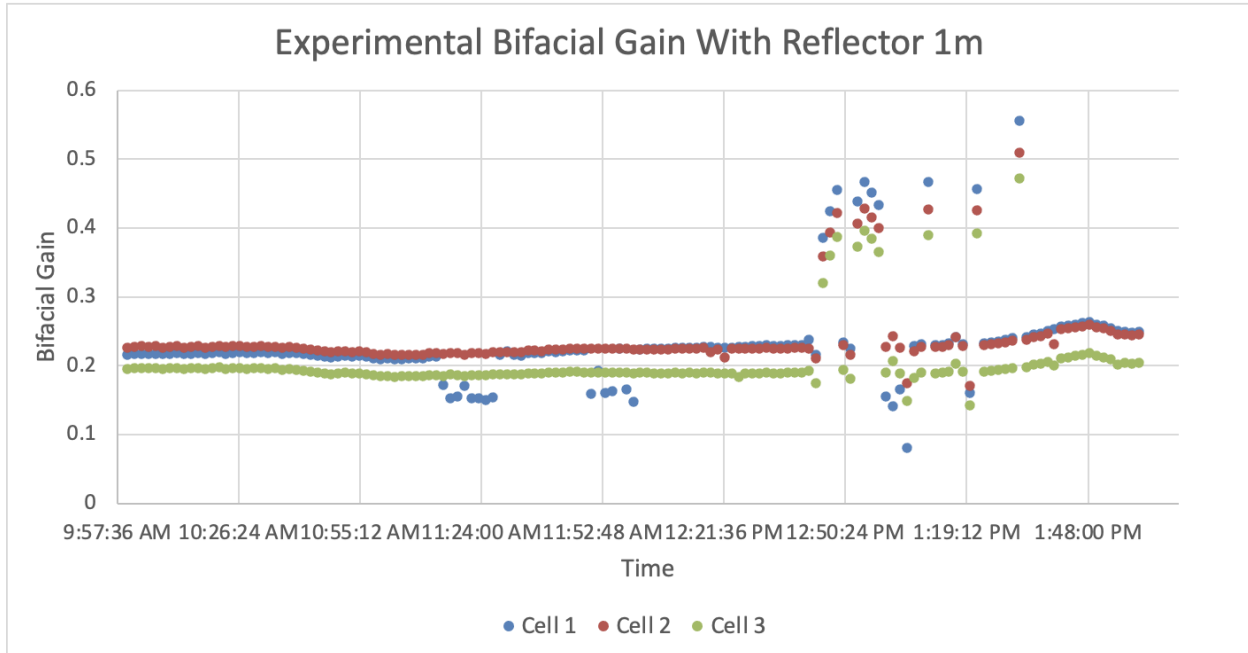


Figure 18: Bifacial gain of 3 cells found experimentally with 1m reflector distance.

In Figure 19, the bifacial gain found through the computational model can be observed at separation distances of 0.5, 0.75, and 1 m. The computational model served the benefit of requiring less time because it can be run and produce results much faster than collecting data from an experiment over the course of several days. The computational model resulted in bifacial gains of around 0.16 for the 1 m separation distance; these values are comparable to the experimental data, verifying the numerical model. The model can then be used to explore what the bifacial gains will be in future studies. Due to the results from outdoor experiments and the numerical model, the optimal reflector distance will most likely be between 0.75 m and 1 m spacing between the reflector and the collector.

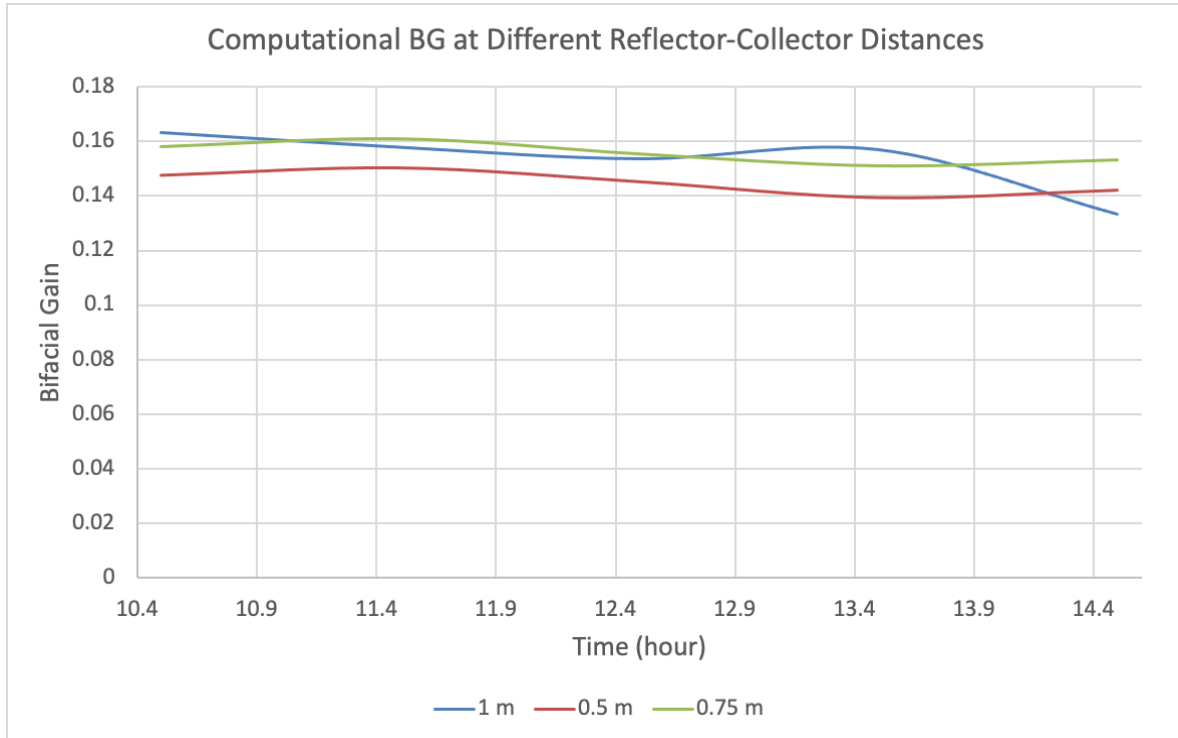


Figure 19: Computational results for the bifacial gain at reflector-collector distances of 0.5, 0.75, and 1m.

The bifacial gain with a white reflector at a reflector-collector distance of 1 m collector over peak solar time from both the experimental and computation model is displayed in Figure 20. The bifacial gain found experimentally was a little over 0.20, so a 20% increase in power generation. While the model predicted a slightly lower bifacial gain of 0.16. While slightly off, the numbers are comparable to results obtained over the summer [9]. The effect of the reflector-collector distance could then be studied using the indoor model. A white reflector was placed at various distances from the rear side of the collector, and the resulting bifacial gains can be observed in Figure 21. The computational model could be adjusted to the same dimensions as the indoor model, and the same reflector-collector distances can be remodeled and graphed in Figure 22.

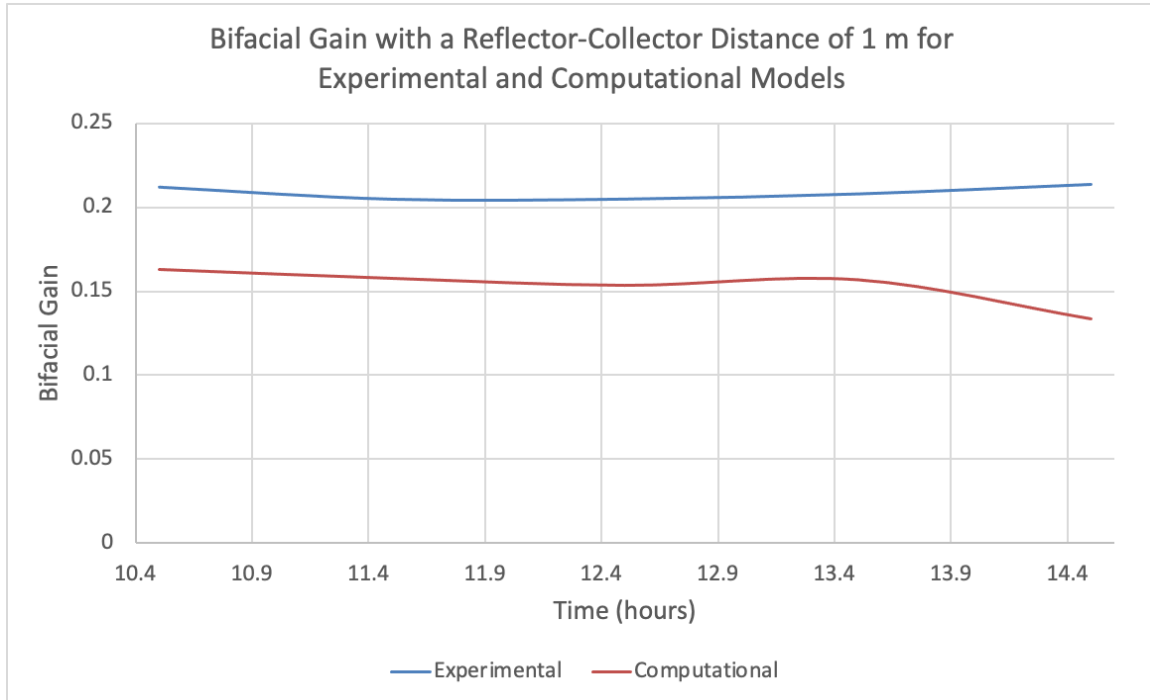


Figure 20: Bifacial gain for a reflector-collector distance of 1 m for the outdoor experimental and computation models.

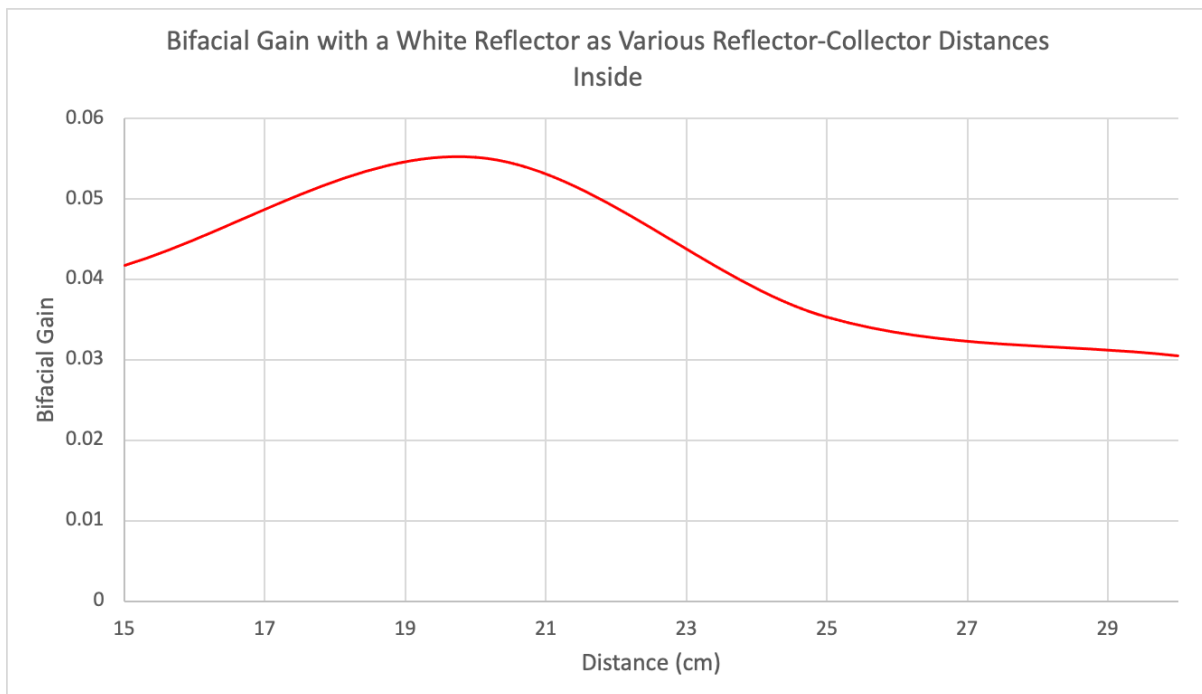


Figure 21: Bifacial gain for several reflector-collector distances from the indoor model.

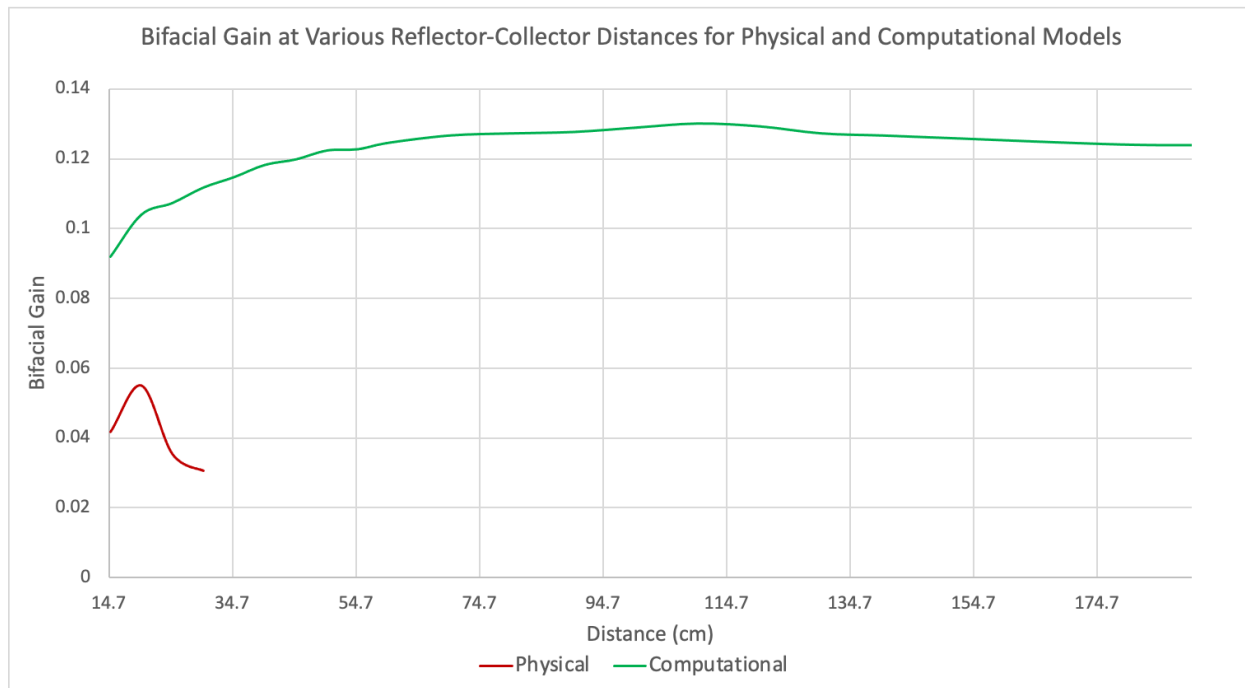


Figure 22: Bifacial gain for various reflector-collector distances showing a peak then plateau for both the indoor and computation models.

For both the indoor and Python models, a peak bifacial gain can be seen at a specific reflector-collector distance. However, this distance is around 20 cm. for the indoor model, and 110 cm for the computational model. While this discrepancy is somewhat high, both models display similar behavior, climbing to a maximum power gain then dropping off and plateauing after. This is a helpful trend to observe and keep in mind.

In addition, for both the outdoor and indoor models, nonuniformity was observed between the top and bottom rows of solar modules. In the outdoor model, the average bifacial gain of the top three modules was 8% higher than the four modules on the bottom row throughout the peak solar hours. The bifacial gain for the top and bottom row of the outside collector can be seen in Figure 23. The top row has a much higher bifacial gain, especially as the sun gets lower in the sky in the afternoon, so less sunlight and diffuse light is reaching the bottom row. While there is a large disparity between the top and bottom row power generation,

the 20% increase in energy captured with the addition of a reflector is significant. In order to claim that the reflector would be worth adding to a bifacial PV array, an actual bifacial model should be tested to see how the nonuniformity caused by a rear side reflector affects the power output.

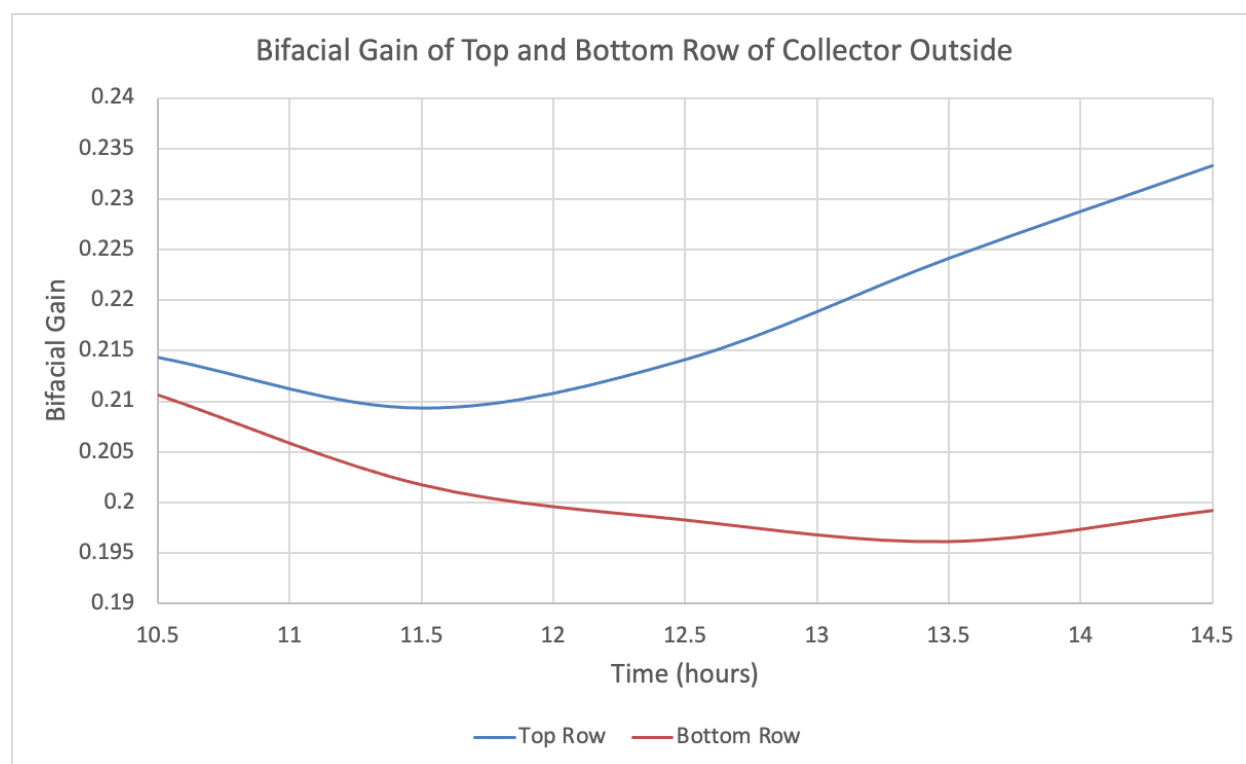


Figure 23: Bifacial gain for top and bottom row of modules over peak solar time with a 1m reflector-collector distance outside.

The average bifacial gain for the two solar modules on the top and bottom row can be seen graphed in Figure 24 for reflector-collector distances from 15 to 35 cm. The top row had an average bifacial gain of 12.3% higher than the bottom row, which is comparable to the results gathered from the outdoor setup. The percent change for each reflector-collector distance between the top and bottom rows can be seen in Table 1. With the largest difference being when the reflector was 15 cm. behind the collector, the shortest distance tested. This is logical because the reflector saw more of the bottom half of the collector the closer together they were.

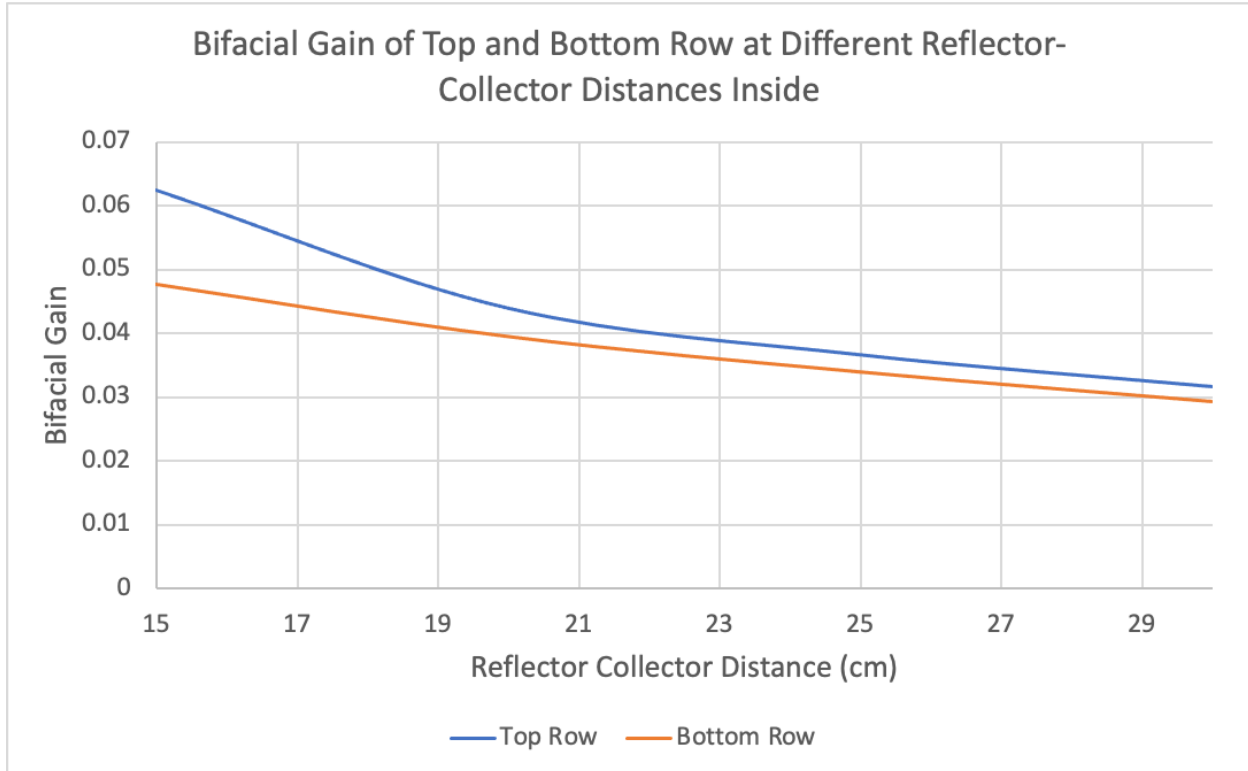


Figure 24: Bifacial gain for top and bottom row of modules over a range of reflector-collector distances inside.

Table 1: Percent increase of bifacial gain between the top and bottom row on indoor setup.

Refl.-Coll. Distance (cm)	% Change Between Top and Bottom Row
15	23.76
20	10.25
25	7.48
30	7.52

The bifacial gain found by changing the reflector distance in the indoor model can then be compared to the computational results as seen in Table 2 and is graphed in Figure 22 above. The computational model had a BG of around double that of the indoor model as explained previously. And the BG from the computational model peaked at a much farther

reflector-collector distance than the indoor model. While the results do not match exactly, the patterns found experimentally can be verified. An optimal reflector-collector distance is confirmed, where the BG then plateaus as the reflector is moved further away.

Table 2: Comparison of bifacial gain for indoor model and computational model at different reflector-collector distances.

Reflector-Collector Distance (cm)	Computational Model BG	Indoor Model BG
15	0.092	0.0551
20	0.104	0.0417
25	0.111	0.0353
30	0.116	0.0305

There are many other parameters that contribute to the arrangement of bifacial PV farms including material of the reflector, the tilt angle of the collector, the addition of a ground reflector, and many others that could not be tested in the time allotted. In the indoor model, it was simple to test many factors in a short amount of time. Initially, a Mylar film reflector was tested against a white reflector at the same reflector-collector distance. While the Mylar film had resulted in a higher bifacial gain at some points, the white reflector was overall more reliable which was seen through data collected by Rueter and Dobosz over the summer, and if a bifacial collector is nonuniformly lit the efficiency can decrease [9]. Next, the reflector was tilted to see the effect on solar energy collected and can be seen in Figure 25. However, as the reflector was tilted backward any less than 90°, or vertical, no increase in bifacial gain was observed. Additionally, the computational model is not able to simulate the tilting of a reflector or collector, so the experimental results could not be compared.

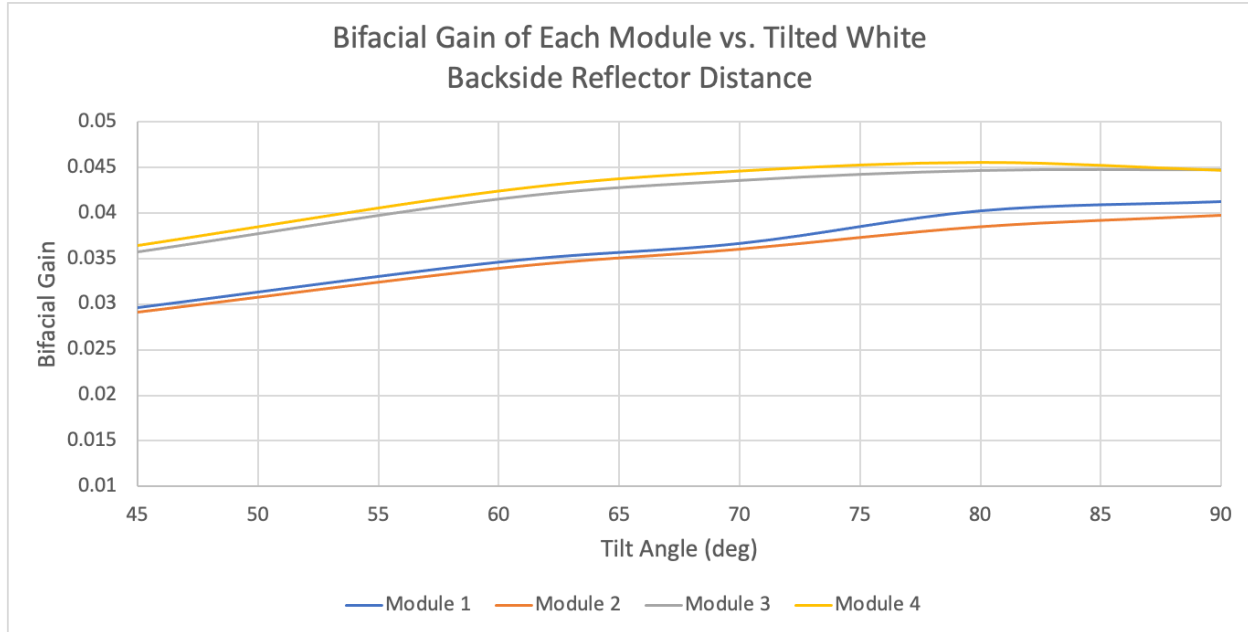


Figure 25: Bifacial gain of each of the four cells as the white rear-side reflector was tilted.

Afterward, a white ground reflector was placed on the ground between the indoor collector and the white reflector. The bifacial gain was then recorded as the vertical reflector was moved back with and without a ground reflector, results shown in Figure 26 and Table 3. When the rear-side reflector was closer to the collector the ground reflector did not make much of a difference, however as the reflector was moved further away, the ground reflector increased the BG by up to 7.5%. For such a minimal addition, a large increase in power gain was observed in the simulated bifacial collector. Overall, more research could be done around bifacial array setups, but there are many additions that could be made to vastly increase power generation.

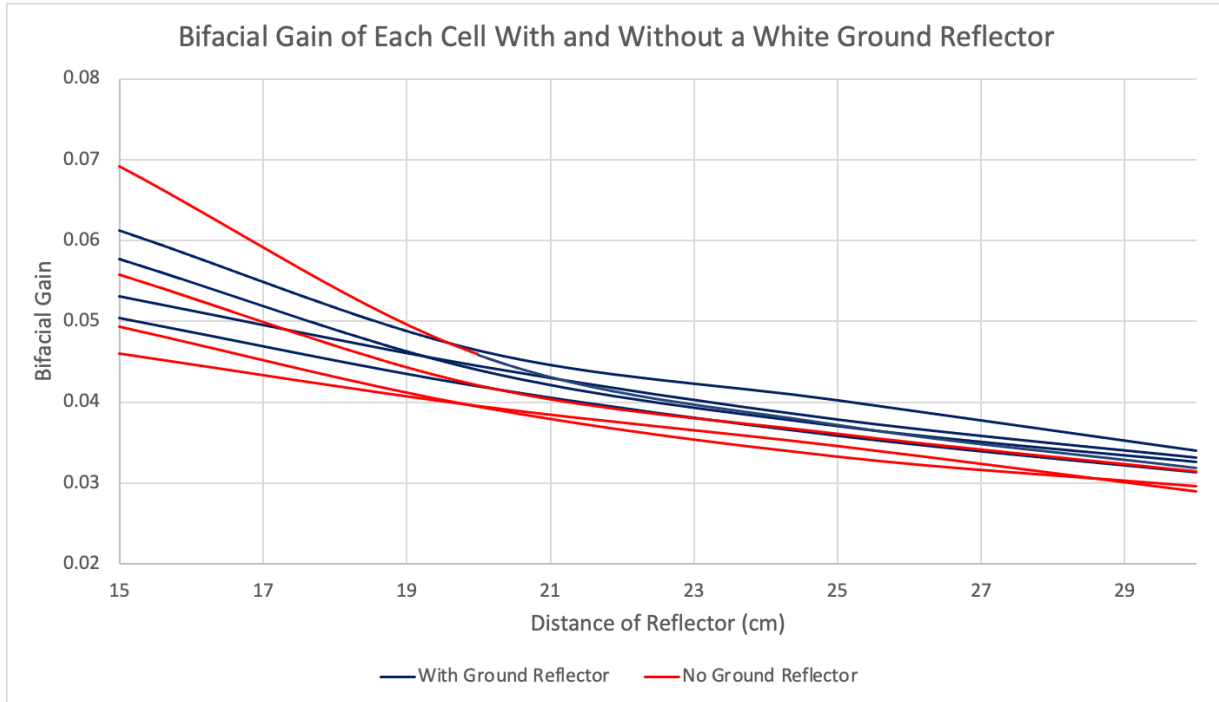


Figure 26: Bifacial gain of each of the four modules with and without a white ground reflector.

Table 3: Bifacial Gain with and without a white ground reflector and percent increase.

Reflector-Collector Distance (cm)	BG With Ground Reflector	BG Without Ground Reflector	% Increase
15	0.0556	0.0551	0.96
20	0.0442	0.0417	5.9
25	0.0378	0.0353	6.9
30	0.0328	0.0305	7.5

Conclusions

Overall, the separation distance between a collector and a backside reflector can be tested through experimental tests done on a rooftop with satisfactory lighting, as well as using a scaled-down indoor model. Experimental data was then used to verify results from the Python computational model. Nonuniformity was observed producing a 10% higher bifacial gain on the top row of solar modules than on the bottom when a rear-side reflector was added. Despite the nonuniformity, from experimental and computational results, the optimal separation distance will most likely be around 1 m based on the outdoor experimental setup, resulting in a significant power gain of 20% over a typical monofacial PV module. The addition of a white ground reflector also had promising benefits that could be applied to just the location of potential bifacial farms.

Several other variables affect the set-up of the bifacial panel and reflector, including the height from the ground and azimuth angle, however, not all factors can be studied due to time and cost constraints. Furthermore, this leaves the opportunity for future studies to be conducted around optimizing for the lowest cost or the most power generated by a module. Many studies have focused on these topics, and solar trackers are often used to automatically adjust panels to face the sun. However, trackers are often not worth the extra cost upfront. Partial shading and nonuniformity are also major problems facing monofacial and bifacial photovoltaic cells. There is minimal data on the non-uniformity of illumination on the backside of panels [6]. As the module elevation is increased, the irradiance uniformity is often improved. However, uniformity could be enhanced even more, as evidenced throughout the experiments in which the addition of a rear-side collector caused non-uniformity among the simulator bifacial “collector”. Some complicated variables could not be recreated experimentally, nor replicated through

computations due to limitations in the Python model. For example, the model is not able to accurately estimate the effects of tilting the reflector and collector. For future studies, the computational model could be improved using an experimental setup and existing literature.

Overall, the use of bifacial PV cells can vastly increase power production over typical monofacial modules. Solar energy is a thriving sector of renewable energy and is able to produce financial returns and reduce greenhouse gas emissions. Bifacial PV is able to further increase energy production by 10-30% over a monofacial cell by collecting solar energy on the front, side, and rear of a collector. Currently, bifacial modules are mostly being used on a commercial scale, usually in power plants or in pilot plants to test their performance [15]. For the future of implementing bifacial PV, some potential adjustments could be a new type of bifacial glass called “AtaMo” changing the thickness and coating of the backing material [15]. There continues to be an abundance of tests and research that could be useful in optimizing bifacial PV manufacturing and array geometry. However, through this study, a successful outdoor and indoor model simulating the rear-side of a bifacial model could be constructed, and the resulting data was validated using an accurate computational model. With a focus on the effect of reflector-collector distance, a peak distance was found to be around 1 m, in which a significant increase in energy was observed to be 20%.

References

- [1] Guerrero-Lemus, R., R. Vega, Taehyeon Kim, Amy Kimm, and L. .. Shephard. 2016. “Bifacial Solar Photovoltaics – A Technology Review.” *Renewable & Sustainable Energy Reviews* 60:1533–49. doi: 10.1016/j.rser.2016.03.041.
- [2] “Bifacial Design Guide - LG Electronics.” [Online]. Available: https://www.lg.com/global/business/download/resources/solar/Bifacial_design_guide_Full_ver.pdf. [Accessed: 26-Oct-2021].
- [3] Rueter, M. “Modeling of Incident Solar Energy on Bifacial Solar Collectors.” *Union College*, 1-32
- [4] Prakash S., Walsh T., and Aberle A. 2014. “A New Method to Characterize Bifacial Solar Cells.” *Progress in photovoltaics* 22, no. 8: 903–909.
- [5] Cuevas, A., Luque, A., Eguren, J., and Del Alamo, J., 1982, “50 Per Cent More Output Power from an Albedo-Collecting Flat Panel Using Bifacial Solar Cells”, *Solar Energy*, Vol 29, No. 5, pp. 419-420.
- [6] Kreinin, L., Bordin, N., Karsenty, A., Drori, A., Grobgeld, D., and Eisenberg, N., 2010, “PV Module Power Gain Due to Bifacial Design, Preliminary Experimental and Simulation Data”, *IEEE*, 978-1-4244-5892-9/10, pp. 2171-2175.
- [7] Sun, X. et al., 2018, Optimization and performance of bifacial solar modules: A global perspective. *Applied energy*. [Online] 212 (C), 1601–1610.
- [8] Khan, M. R. et al., 2017, Vertical bifacial solar farms: Physics, design, and global optimization. *Applied energy*. [Online] 206 (C), 240–248.
- [9] Rueter, M., Dobosz, M., 2021, “A Study of Reflector-Enhanced Bifacial PV.” *Union College*, 1-13

- [10] Appelbaum, J., 2016. Bifacial photovoltaic panels field. *Renewable Energy*. 85, 338-343.
- [11] Guo, S., Walsh, T.M., Peters, M., 2013. Vertically mounted bifacial photovoltaic modules: A global Analysis. *Energy*. 61, 447-454.
- [12] Lopez-Garcia J., Casado A., and Sample T., 2019, “Electrical performance of bifacial silicon PV modules under different indoor mounting configurations affecting the rear reflected irradiance,” *Solar Energy*, vol. 177, pp. 471–482.
- [13] Jäger, K., Tillmann, P., and Becker, C., 2020, “Detailed illumination model for bifacial solar cells”, *Optics Express*, Vol. 28, No 4, pp. 4751-4762.
- [14] “2.11 collector orientation,” *2.11 Collector Orientation | EME 810: Solar Resource Assessment and Economics*. [Online]. Available: <https://www.e-education.psu.edu/eme810/node/576>. [Accessed: 07-Mar-2022].
- [15] A. Zurita, A. Castillejo-Cuberos, M. García, C. Mata-Torres, Y. Simsek, R. García, F. Antonanzas-Torres, and R. A. Escobar, 2018, “State of the art and future prospects for solar PV development in Chile,” *Renewable and Sustainable Energy Reviews*, vol. 92, pp. 701–727.

Appendices

Appendix A: Cell Calibration Curves

Outdoor:

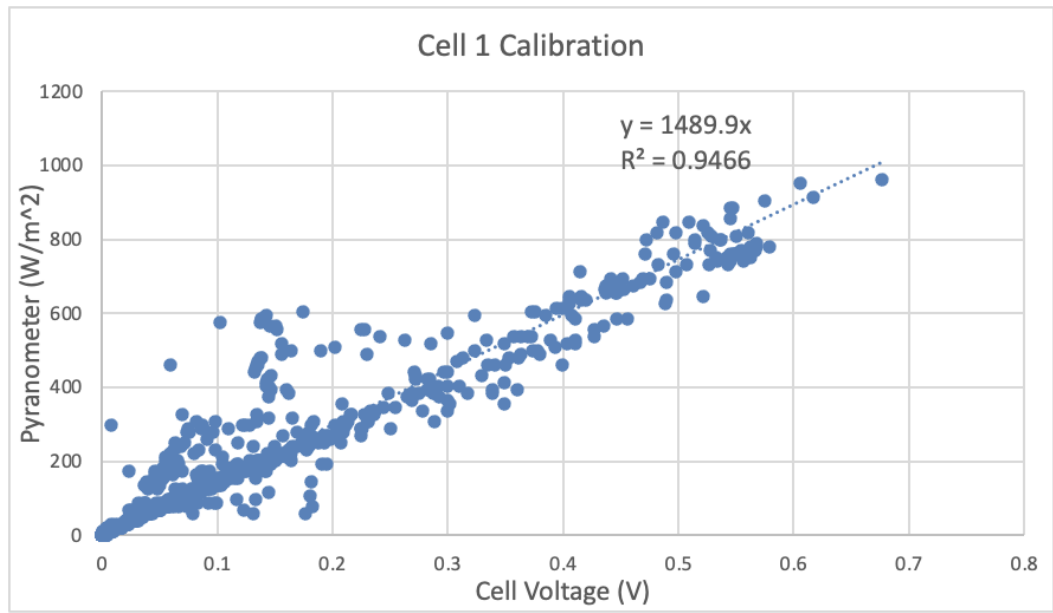


Figure A1: Calibration of Cell 1

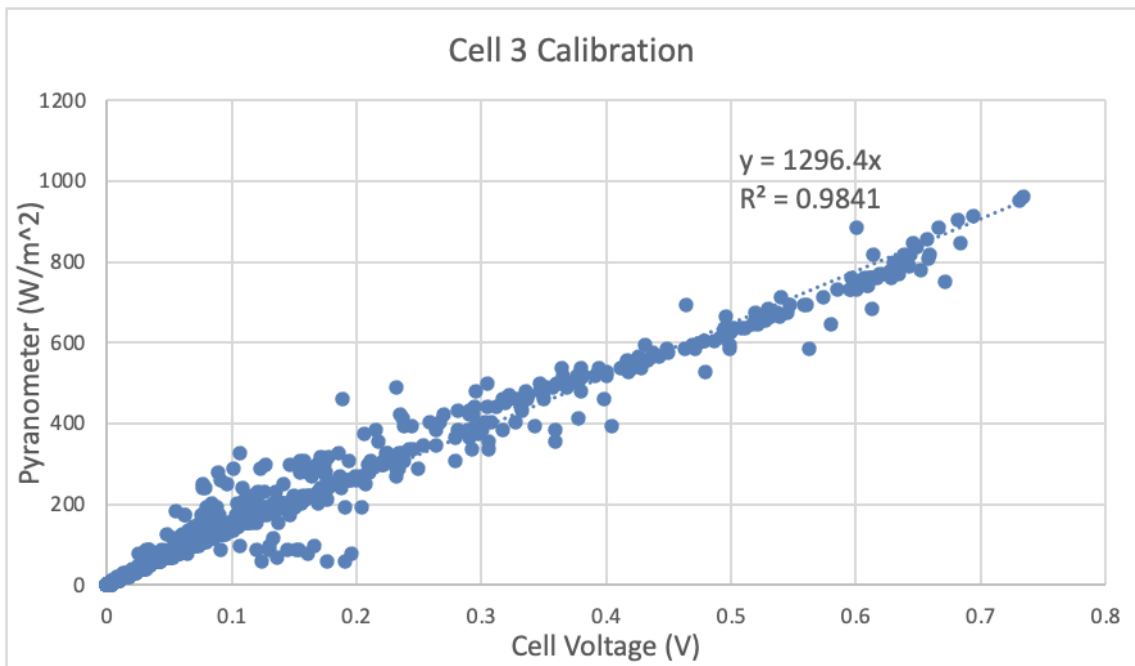


Figure A2: Calibration of Cell 3

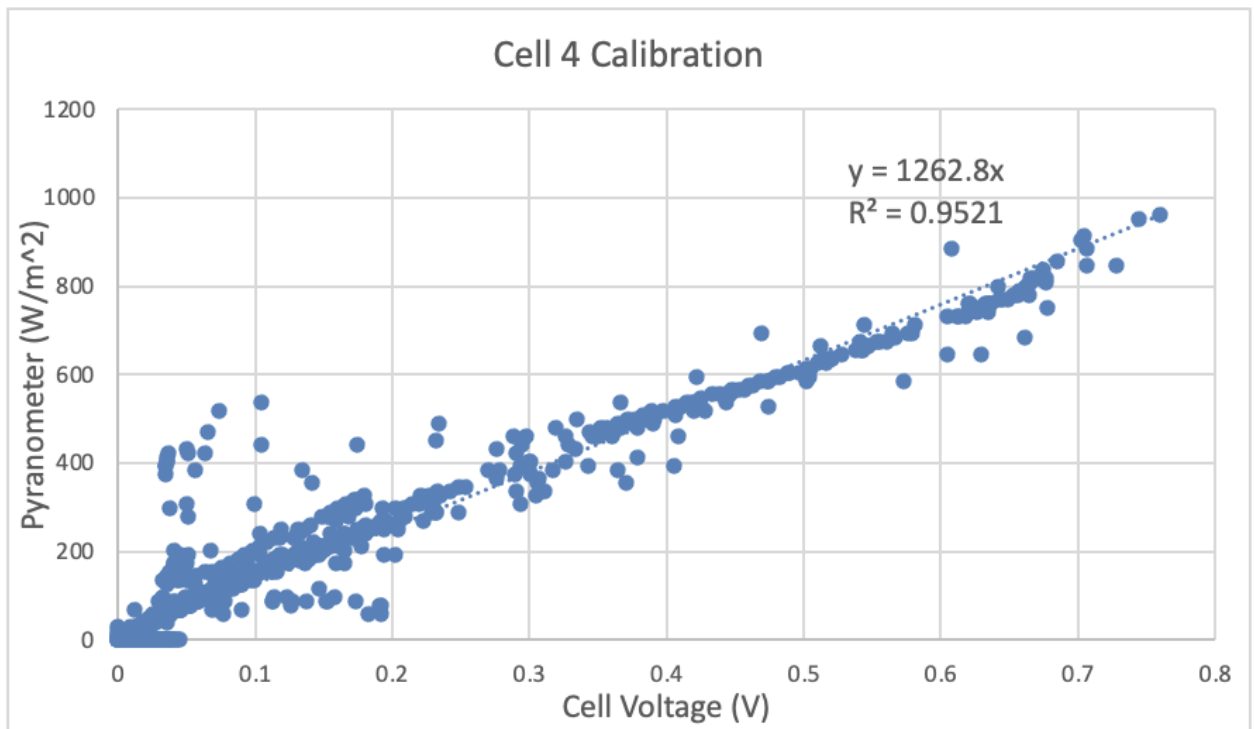


Figure A3: Calibration of Cell 4

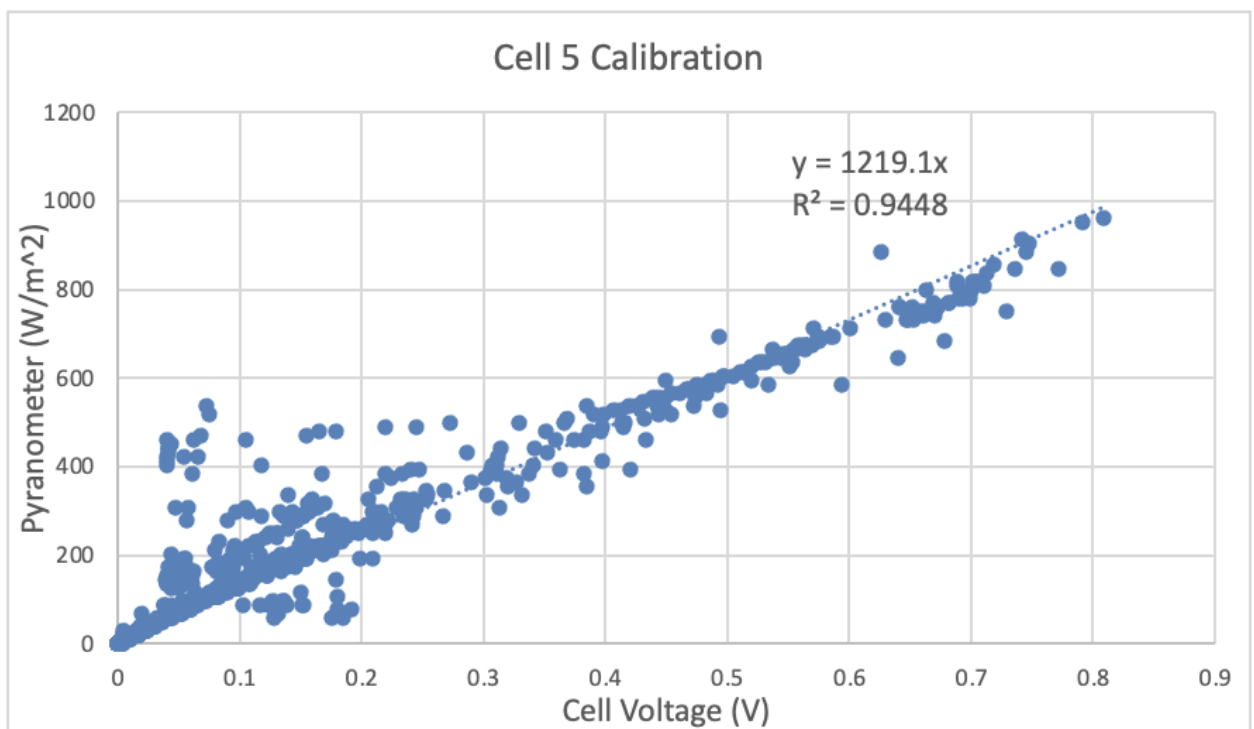


Figure A4: Calibration of Cell 5

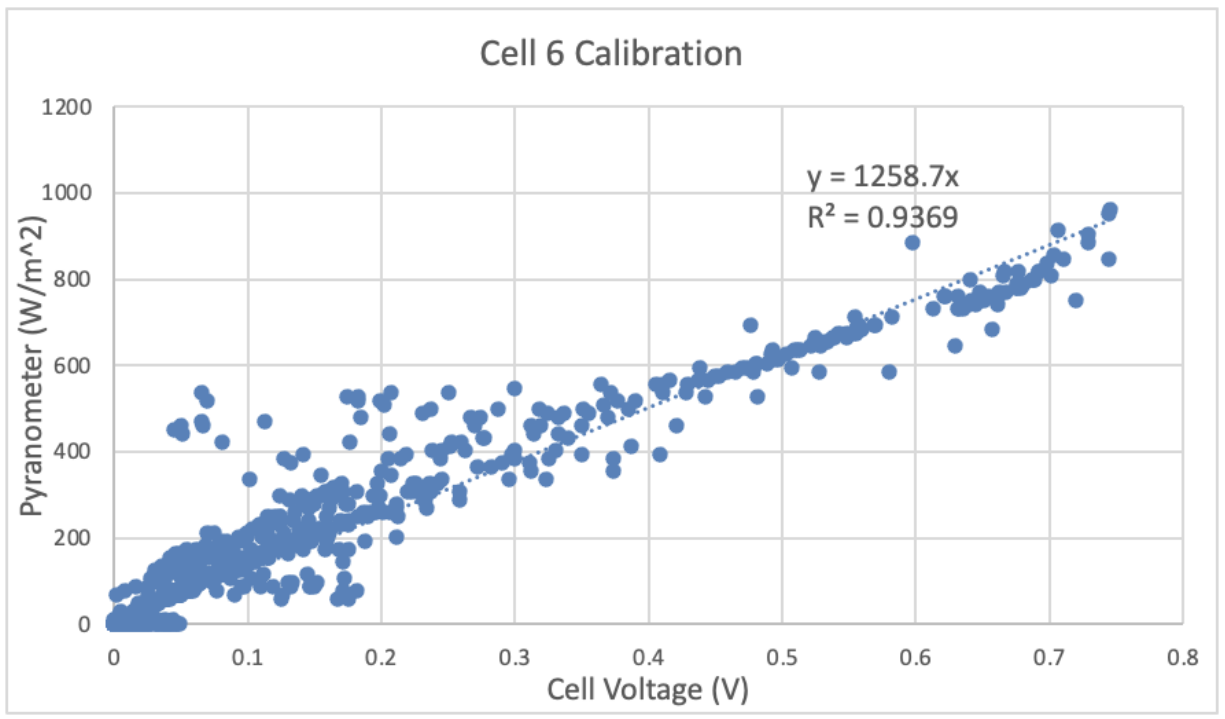


Figure A5: Calibration of Cell 6

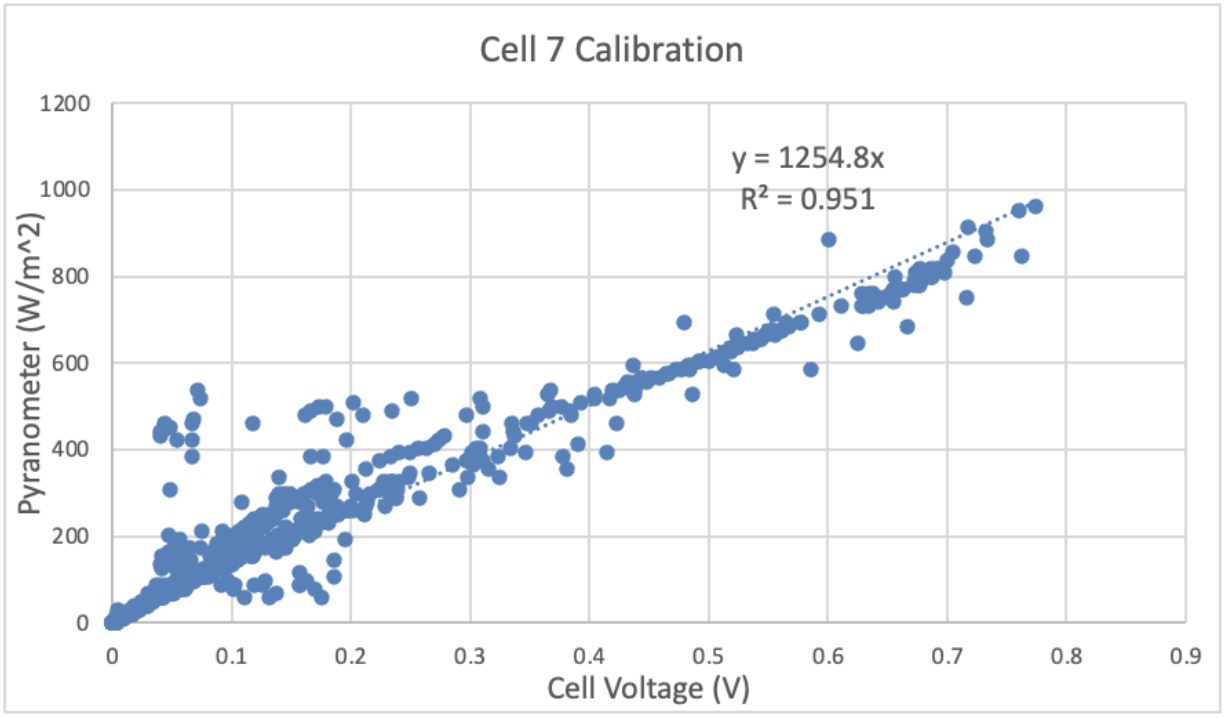


Figure A6: Calibration of Cell 7

Indoor:

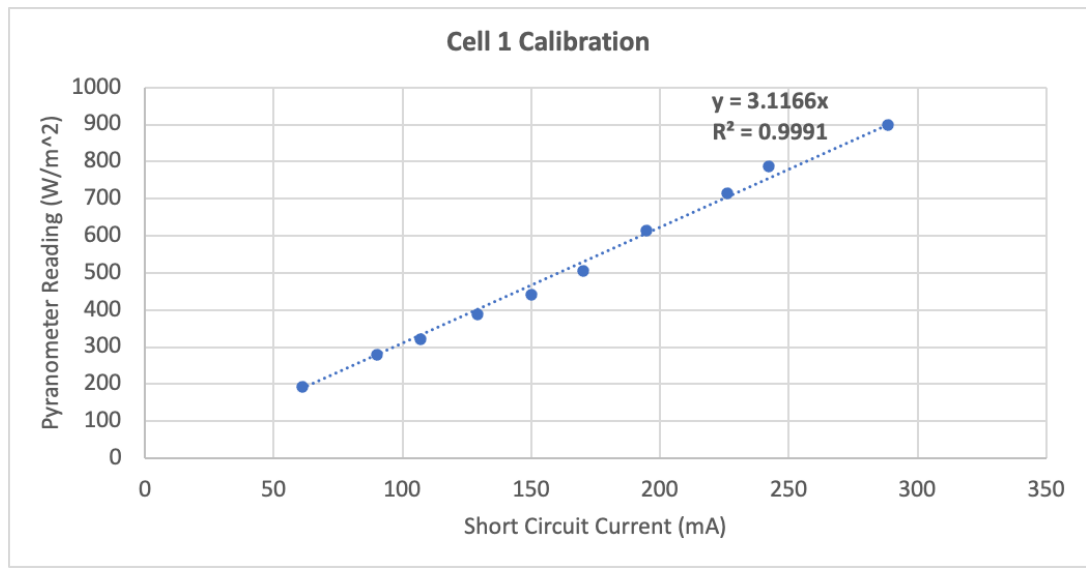


Figure A7: Cell 1 Calibration Indoor

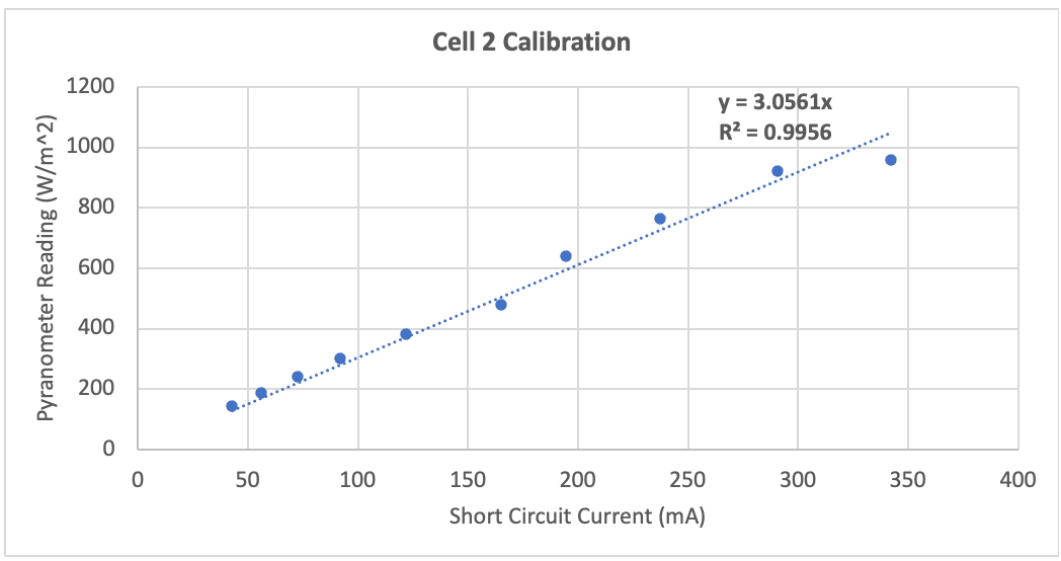


Figure A8: Cell 2 Calibration Indoor

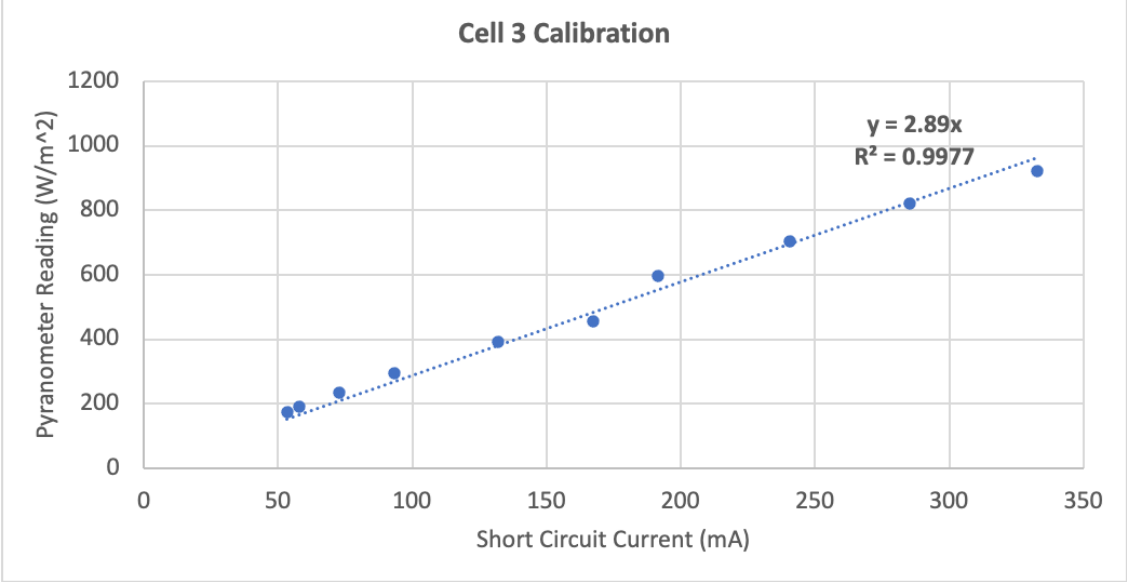


Figure A9: Cell 3 Calibration Indoor

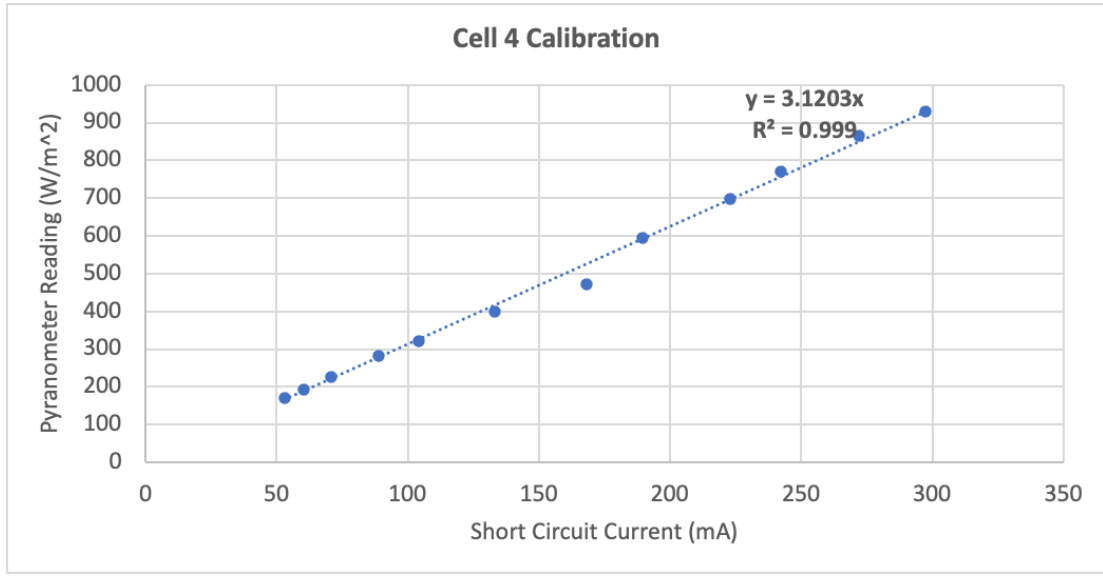


Figure A1: Cell 4 Calibration Indoor